JMEPEG (2023) 32:5731–5740
https://doi.org/10.1007/s11665-023-08181-0

1059-9495/$19.00

TECHNICAL ARTICLE

Microstructural and Mechanical Characterization of Interfacial Phenomena Occurring in Brazing Ti-6AL-4V Alloy Using TiZrCuPd Amorphous Ribbons

Anna Sypien

Submitted: 30 December 2022 / Revised: 25 March 2023 / Accepted: 2 April 2023 / Published online: 20 April 2023

The brazing technology with the proper choose of the filler metals should provide a solution for the major disadvantage of titanium alloys related to the problems of joining. This work concerns brazing of the Ti-6Al-4 V substrates with the originally amorphous TiCuZrPd ribbon. The TiCuZrPd filler enables proceeding of the brazing process below the melting temperature of the alloy, at about 880 °C. As the high quality of the filler/substrate interconnection remains substantial for the industrial application, the evolution of the mechanical and structural properties was studied while the induction and resistance heating were used to obtain Ti/Ti joints. The microstructure studies showed that at the interfaces obtained by both methods, the brazed zone was characterized by the uniform microstructure without defects such as separation of intermetallic phases or Kirkendall voids. In both cases, the interface consisted of three zones: upper diffusion zone, filler material zone and lower diffusion zone. It was also observed that regardless of the heating method used, the width of the reaction zone of the joints was similar, about 47 μm. On the other hand the ratio of the widths of the different zones was altered in dependence on the heating method used. The results showed that the brazing by induction heating increased the shear strength of the tested joints by two to three times, depending on the content of palladium in the filler metal. The highest value of shear resistance of approx. 650 MPa was noted for the joints obtained by induction heating at 850 °C.

Keywords amorphous ribbon, brazing, induction heating, interface, resistance heating, titanium alloys

1. Introduction

Welding and brazing are the most common joining techniques applied in the industrial production for titanium and its alloys. Welding usually influences the microstructure of the joined materials (heat affected zone). In contrast, brazing has less impact on the microstructure and properties of base metal. Titanium alloys play an important role in many modern industries and the most popular is the alloy Ti-6Al-4 V (Grade 5), which generates many problems during its joining with dissimilar materials. Brazing temperature is an important processing parameter because too high temperature leads to the formation of phases what negatively affect the integration of the joint. It is preferred that joining processes were carried out at a temperature lower than β phase transformation of the matrix (~ 1000 °C) (Ref 1).

In the contemporary technology of liquid-assisted joining dissimilar materials by brazing, interfacial phenomena strongly affect structure-properties relationships of the brazed joints. In case of titanium alloys, the thermophysical properties determine important parameters of the brazing process such as temperature, time and number of cycles (Ref 2, 3). The limitations in design of technology of joining titanium alloys result from the changes in the structure and properties which occur above the temperature of the $\alpha + \beta \rightarrow \beta$ phase transformation (Ref 4, 5).

Vacuum brazing of the Ti-alloy uses filler metals that are usually alloyed at a lower melting point with alloys such as Ti-Cu alloy or Ti-Zr-Ni-Cu alloy (Ref 6-9). A low melting point facilitates brazing, however, it also lowers the high-temperature performance of the joints.

(Ref 10). Furthermore, as brazing temperature increased, the growth of interfacial Cu-Ti intermetallic compounds greatly deteriorates the shear strength of the joint. Chang (Ref 11) brazed titanium alloy using Ti-15Cu-15Ni and Ti-15C-25Ni filler metals. The joint fractured along the Cu-Ni-rich Ti phase. Therefore, when the joint is subjected to the uniaxial tensile loading, cracks originate and causes premature joint failure (Ref 12-17) in the brittle Cu-Ni-rich Ti phases in the joint.

Despite the fact that numerous compositions of the brazing filler metals have already been tested, there is still no filler metals for brazing of titanium alloys produced for commercial markets at processing temperature above 800 °C (Ref 10, 18).

The promising group of materials, which can be used as a brazing material to join Ti alloys are metallic glasses (Ref 19,

This article is an invited submission to the *Journal of Materials Engineering and Performance* selected from presentations at the 10th International Conference on High-Temperature Capillarity (HTC 2022) held September 12-16, 2022, in Kraków, Poland. It has been expanded from the original presentation. The issue was organized by Prof. Natalia Sobczak of the Polish Academy of Sciences.

Anna Sypien, Institute of Metallurgy and Materials Science, Polish Academy of Sciences, Reymonta 25 St., 30-059 Krakow, Poland. Contact e-mail: a.sypien@imim.pl.

20). The amorphous alloys, in comparison with the crystalline metallic materials, reveal unique physical, chemical and mechanical properties due to their amorphous structure, which does not contain defects of the crystalline structure such as dislocations and interphase boundaries. Their properties allow the production of brazing filler metals in the form of thin, ductile flexible ribbons 20-100 μm thick from alloys. In addition, a filler material in the form of ribbon is easier to apply and it does not contain organic impurities that are found in solder pastes and powders. The advantage of amorphous ribbons consists in their higher chemical homogeneity even after crystallization, as well as the narrow temperature range of the phase transformations and melting. The intention in using amorphous brazing filler metals is not only to achieve strong brazed joints, but also to save the energy on heating and reduce brazing time, which are very important for brazing in modern industry. A combination of vacuum brazing and amorphous filler metal could be an alternative method to manufacture a joints of Ti-6V-4Al (Grade 5) titanium alloy with sufficient strength and minimal distortion. For demonstrating the effect of using amorphous strips for soldering, induction and resistance heating were used.

Electromagnetic induction is a method of heating electrically conductive materials. Commonly used processes are heating prior to the metal working, heat treatment, materials joining and melting. In the case of induction heating the flow of ac current through the coil generates an alternating magnetic field which cuts through the workpiece. This alternating magnetic field induces the eddy currents that heat the workpiece. Induction heating finds application in the metals-processing industries. Induction brazing and soldering also involve the local heating and these processes can be precisely controlled by of heating and cooling rates (Ref 21). Induction brazing in an inert gas or vacuum atmosphere can be used successfully for joining titanium and its alloys. Induction brazing of small, symmetrical parts is very effective (Ref 22). The application of induction heating technique in a brazing process allows obtaining higher heating rates and smaller amount of oxidation, distortion and grain growth in the parent materials, as the joint area remains at an elevated temperature for a short time (Ref 23). However, high temperature of heating in solids is often accompanied by diffusion and structural phase transformations. These processes are interconnected and interdependent: diffusion of the elements can stimulate structural phase transformations, and the latter change the conditions of diffusion. It is difficult to describe these processes analytically (Ref 24).

This work is focused on the possibility of using Ti-based filler metal in the form of amorphous ribbon for brazing titanium alloys at temperatures near 800 °C. The goal of this study is to characterize the joint microstructure of the commercial Ti-6Al-4 V titanium alloy which was brazed in the resistance furnace or by induction heating in a controlled atmosphere with application of a new type of amorphous brazing foils (Ti40-Zr10-Cu36-Pd14, at. %). The paper presents the comparison of the microstructures of the joints obtained by two different brazing methods using amorphous ribbons with addition of palladium, as a filler metal. It was assumed that the use of amorphous ribbons as fillers will enable to obtain defect-free and high-strength joints at temperatures reduced to about 800 °C. The results allowed to describe the relations between structure of the joint and its mechanical behavior under various testing conditions (temperature, brazing method). It was showed that the amorphous Ti-Cu-Zr ribbons with addition of palladium can be treated as a perfect candidate for the filler metal to joint.

Ti-6Al-4 V alloys. Furthermore, the use of amorphous ribbon as a bonding material without the need of a flux, allowed to obtain a homogeneous, porosity-free joints of high quality and mechanical strength.

2. Experimental

2.1 Materials and Brazing Technology

Ti-6Al-4 V alloys (Grade 5) in a sheet form with the thickness of 3 mm was used as brazed substrate. The substrates had dimensions of 4 mm in width and 20 mm in length. Filler metal was in the form of amorphous foil with a thickness of 0.05 mm and width of 4 mm, produced by a melt spinning process on the rotating disc with a rate of 43 m/s.

The Ti40-Cu36-Zr10-Pd14 (Pd-14) alloy was prepared from a high-purity components by cold crucible levitation melting under the argon at atmosphere (Ref 25).

Figure 1 shows DSC curves revealing the crystallization process of the amorphous ribbons at low (30 °C/min) and high heating (100-140 °C/min) rates. The results allowed establishing that the crystallization proceeds in two stages for the Pd-14. The vitrification temperatures T_g was within a range of 437-51 °C the temperatures of the primary crystallization T_{x1} was 465-485 °C, and for the secondary crystallization T_{x2} = 548-561 °C. The increase in characteristic temperatures T_g and T_{x1} was responsible for improving the alloy ability to form the metallic glass. It was shown that application of the low heating rate led to the shifting of the thermal effects of crystallization toward lower temperatures by about 20°, indicating the relation between crystallization and diffusion. Additionally for the 30 °C/min heating rate, widening of the thermal effect was observed, which was due to the crystallization of at least two phases in the overlapping temperature ranges.

Two brazing processes were designed in this study. The processing temperature was determined from the Differential Scanning Calorimeter (DSC) analysis and wetting tests (Ref 26, 27). The first brazing trial was made in a resistance furnace, at two temperatures, 850 and 880 °C and with annealing for 5 min. In this case the heating rate was 31 °C/min, while the cooling was 7 °C/min. In the second brazing method the induction heating was applied, done in three stages. In the first and the second stages, the temperature was increased up to 600 and 700 °C, respectively, followed by the annealing for 30 s. The applied heating rates were 533 and 100 °C/min. The brazing was realized in the third stage, which was conducted at three temperatures: 790, 810 and 850 °C, with 1-min annealing. The cooling proceeded with the 70 °C/min rate.

For this process, an induction coil was especially prepared. The shape of the coil was similar to the shape of the samples. The homogeneous temperature in the whole volume of the sample was confirmed by the use of a thermal imaging camera. Before brazing, the substrates were polished with the sandpaper 1000, then ultrasonically cleaned in ethanol and dried in air. Once the furnace was closed, it was evacuated and flushed with the protective gas, three times before heating was started. During the tests, a flow of Ar-15 vol. % H_2 gas mixture was

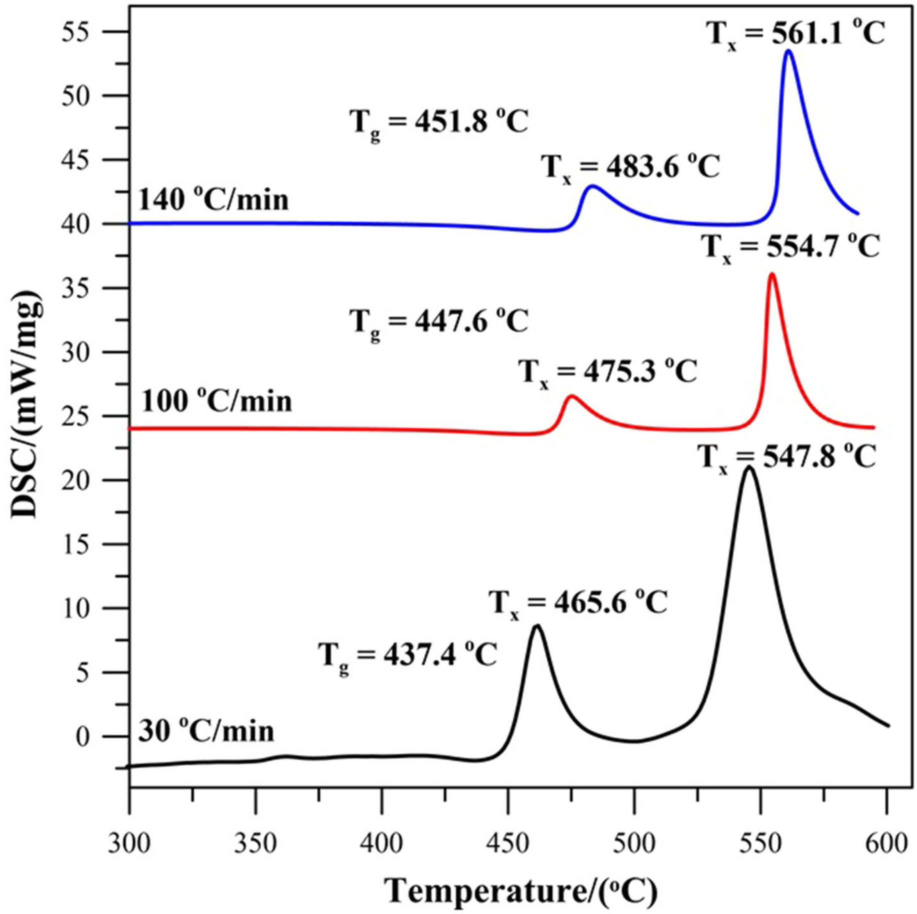

Fig. 1 Comparison of the DSC curves recorded during the heating cycle for the Ti40Cu36Zr10Pd14 amorphous ribbon, applied low 30 °C/min (DSC Netzsch F1 Pegasus) and high heating rates 100 and 140 °C/min (DSC Netzsch 214 Polyma)

maintained. The lap joint design was employed for the brazing process.

2.2 Microstructure Characterization

The microstructure of the joints was characterized with aims of the scanning electron microscope FEI Quanta 3D FEGSEM (SEM) and energy dispersive x-ray spectroscopy (EDS) EDAX Trident system and the transmission electron microscope Tecnai G2 F20, 200 kV (TEM). The electron diffraction in TEM was used to identify phases formed in the joining process.

2.3 Mechanical Properties Testing

To characterize the mechanical properties, the joints were tested for the shear strength using a specially designed holder, at room temperature. For joints obtained by induction heating, the shear tests were carried out for all three brazing temperatures, 790, 810 and 850 °C. For joints obtained by the resistance heating two brazing temperatures 850 and 880 °C were used. Three samples for each brazing condition were used for shear tests at room temperature. Finally, after the shear test, the structure characterization of the fracture surfaces was carried out.

3. Results and Discussion

3.1 Effect of Brazing Process on the Microstructure of the Joint

Figure 1 shows the comparison of the joint structures formed at 850 °C/5 min by using induction and resistance heating. The brazing zone was characterized by the uniform microstructure without defects such as separation of the intermetallic phases, discontinuities or Kirkendall voids. In both cases, three zones were observed at the interface: upper diffusion zone, brazing material zone and lower diffusion zone. It was also observed that regardless of the heating method used, the width of the reaction zone in the joint was similar, about 47 μm. On the other hand, the width ratio of the different zones changed, depending on the heating method used. In the case of the resistance furnace brazing, the widest zone was the brazing material zone (about 27 μm), and the two diffusion zones revealed the same width of about 9 μm (Fig. 2a). After induction brazing, a narrowing of the braze zone to 9 μm and an increase in the width of both diffusion zones to 20 μm were observed (Fig. 2b). In both cases, a continuous layer of intermetallic phase was noted on both sides of the filler material. Their thickness was about 4 μm for the resistance heating, while for the induction heating it was smaller, about 700 nm (Fig. 2c-d). These differences are mainly due to the fact, that the process of induction heating is more dynamic and

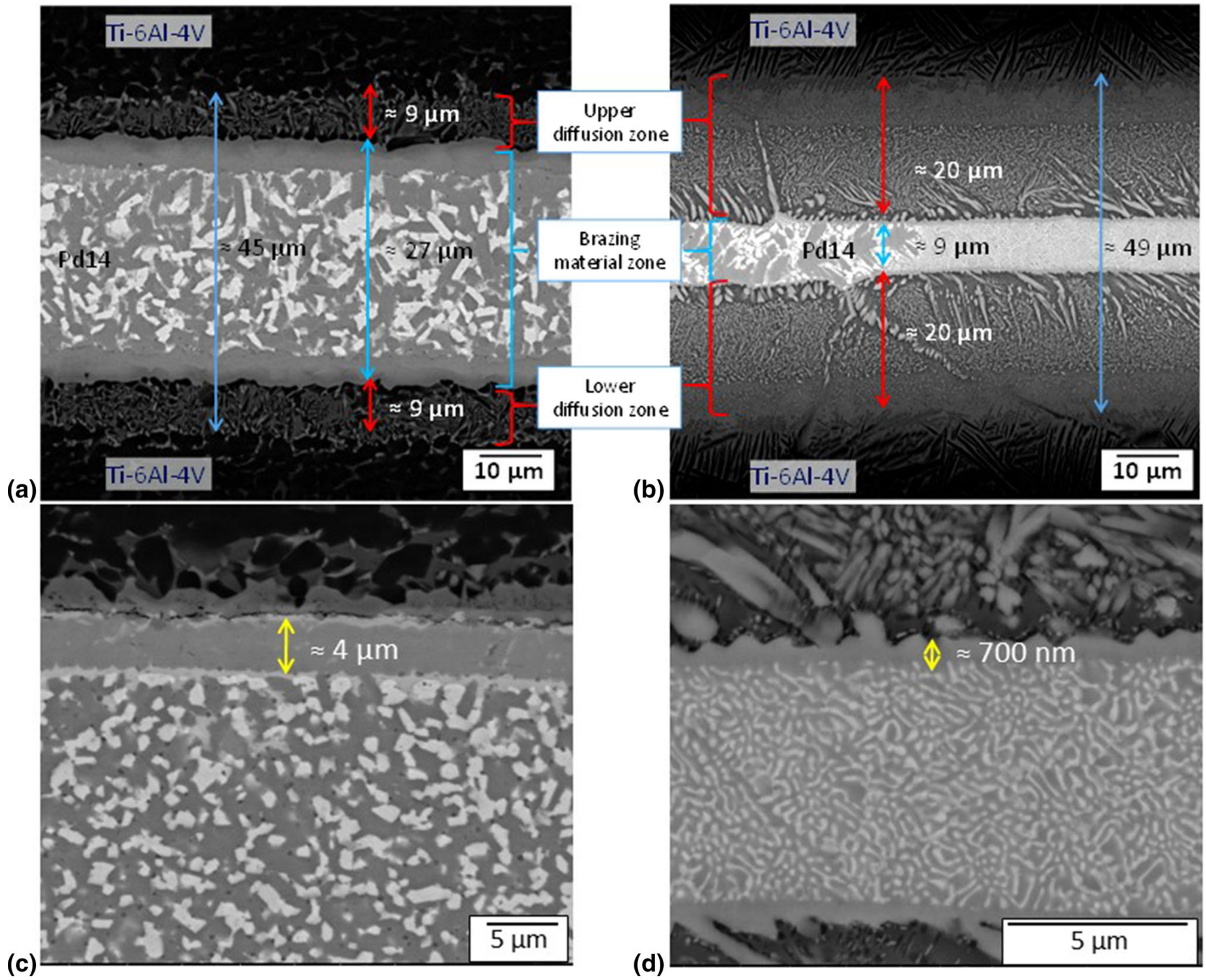

Fig. 2 Cross section microstructure of the Ti-6Al-4 V/TiCiZrPd/Ti-6Al-4 V joint obtained by used two different brazing methods at 850 °C for 5 min annealing: (a,c) resistance heating, (b,d) induction heating

causes higher temperature gradients in the individual zones of the joint. In addition, rotary currents influence the processes of diffusion occurring in the reaction zone.

TEM studies showed that in the joint reaction zone three layers were formed after the resistance heating (Fig. 3). In the middle reaction zone noted as 4, the complex structure of multiple phases was observed in which mainly tetragonal CuTi phase, enriched in Pd was detected (Fig. 3b). The electron diffractions, acquired from different areas (marked as 1-4 in Fig. 3b) confirmed the additional five phases: Cu_3Ti_2, PdZr, Pd_3Ti, $CuZr_2$ and CuTiZr.

The layer noted as 1 was composed of a tetragonal $CuTi_3$ phase, in the form of elongated bright needles (STEM-HAADF, shown in Fig. 3c) by the red arrow, and a matrix of the composition very close to the applied substrate (area 3). The layer 2, a very thin continuous layer marked as $CuTi_2$ phase was enriched in Pd and layer 3 next to the solder, was composed of the tetragonal CuTi phase enriched in Pd and Zr. This layer was formed as a result of intense reaction between the filler material and the substrate, with the composition corresponding to $[Ti,(Zr)_2(Cu, Pd)]$. The results of STEM/EDS analysis suggest that in the reaction zone occurs the intensive diffusion of the elements. The maps of elements distribution (Fig. 3b-c) evidenced that copper, palladium, and zirconium diffused toward the substrate, while aluminum and vanadium in the opposite direction. These results are consistent with the investigations of the crystallization process of amorphous ribbons. Recently, crystallization process in TiCuZrPd amorphous fillers was studied up to ~ 600 °C with DSC, with heating rates 5 and 20 °C/min (Ref 26). This confirmed that at the higher heating rate the crystallization temperature is shifted to higher temperatures. From the XRD and TEM investigations at temperatures close to Tx_1 the phases Cu_2Pd, Cu_8Zr_3 and $CuTi_2$ were evidenced in the joint (Ref 28). The existence of CuTi, $CuTi_2$, Cu_3Ti_2, Cu_8Zr_3, Cu_3Pd, CuTiZr and PdTi, PdZr, Pd_3Zr, Ti_2Zr phases was confirmed at temperature above the secondary crystallization (Ref 28).

In the case of induction brazing, the presence of 3 reaction layers was observed on both sides of the interface. Figure 4 shows the microstructure of the cross section Ti-6 V-4Al/TiCuZrPd joint. TEM/SAED studies and the map of the elements distribution exhibited the layered structure, starting from the substrate side (Fig. 4a). SADPs indicate that after induction brazing, the diffusion zone was composed of two

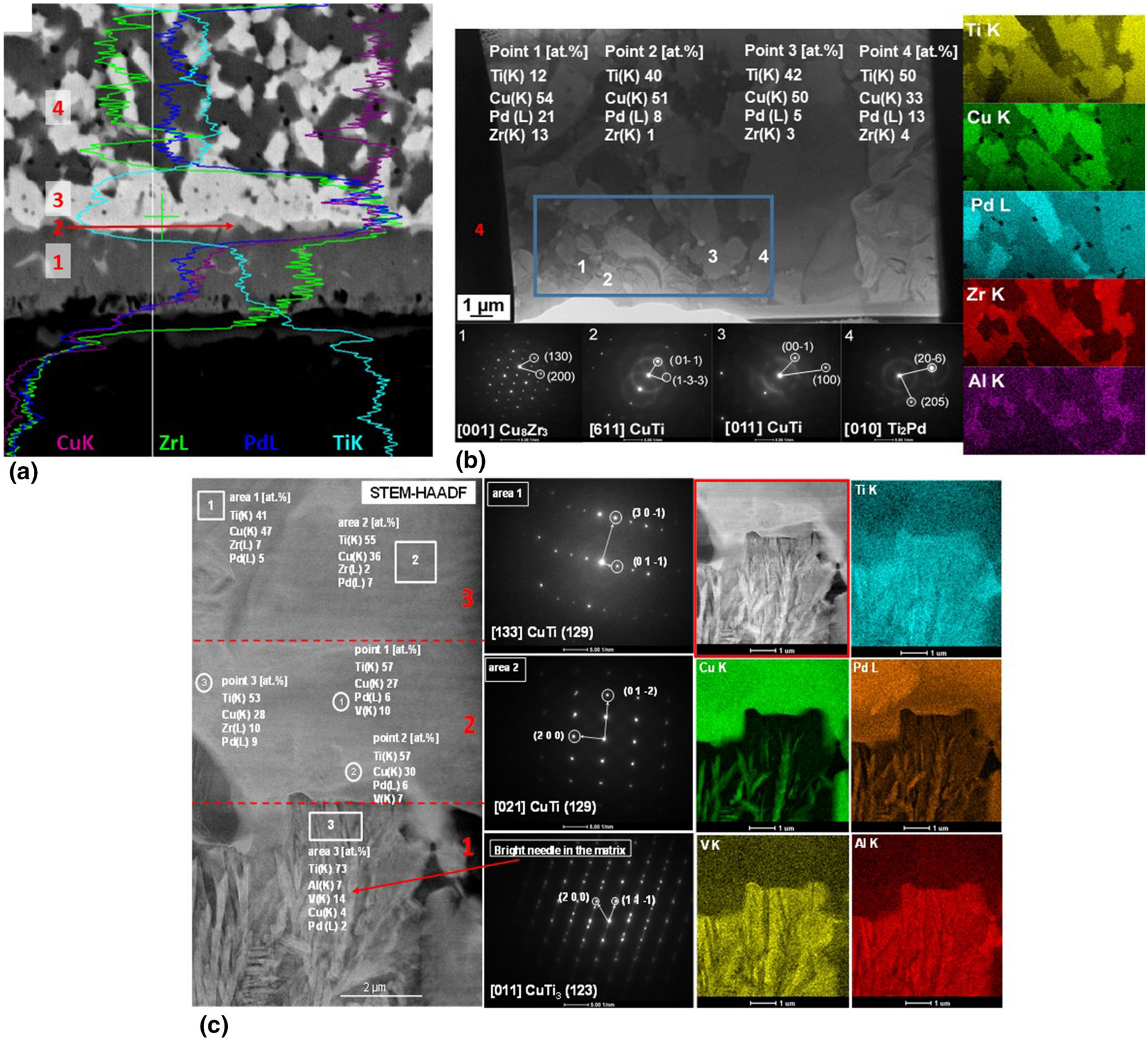

Fig. 3 Microstructure of the interfaces of the Ti-6Al-4 V/TiCiZrPd/Ti-6Al-4 V joint obtained by resistance heating at 850 °C for 5 min: (a) SEM images with marked reaction zones, (b) TEM images, STEM-HAADF, SAED patterns and maps of elements distribution in the central part of the joint, (c) TEM images, STEM-HAADF, SAED patterns and maps of elements distribution at the substrate side

phases (Cu, Pd)Ti_2 and CuTi. The layer revealing decreased Ti and increased Zr content was separated by the layer with reverse Ti and Zr content (Fig. 4b). Moving to the center of the joint, the CuTi phase in the form of elongated sticks was observed (Fig. 4c). Small precipitates revealing TiZr composition were visible between them (Fig. 4a). The (Cu, Pd)Ti_2 phase composed the intermetallic layer, while the central zone of the joint contained the combination of three phases whose chemical compositions correspond to the (Cu, Pd)$_2$Ti, CuTi and CuTiZr phases. TEM studies did not show crystallization of the brittle Laves phase in the intermetallic layer, the presence of which could significantly reduce mechanical properties of the joint.

Recently, the crystallization amorphous ribbon was studied at relatively high rates of heating and cooling (60, 100 and 140 °C/min) (Ref 32). The analysis of the results showed that the process of multiphase crystallization observed at low heating rates became reduced to the crystallization of only the CuTi phase at high rates. The existence of only one phase during crystallization at high heating rates may be explained by the fact that the main components of the alloy are Ti and Cu atoms. Their presence is statistically the most probable in the vicinity of neighbors in a disordered amorphous matrix, which decreases the required distance of diffusion. It was also confirmed that the crystallization of CuTi phase was the most thermodynamically and kinetically favorable process (Ref 29).

Other filler materials used for brazing, with the high strength and corrosion resistance include.

Ti-Zr-Ni-Be, Ti-Zr-Cu-Ni-2 (Ti-38Zr-15Cu-15Ni), Ti-Zr-Cu-Ni-Pd (Ti-37Zr-12Cu-12Ni-2Pd) and Ti-Cu-Ni-2 (Ti-20Cu-20Ni) alloys (Ref 30). Lugschneider and co-authors (Ref 31) proved that mechanical properties of Ti-6Al-4 V and CPTi joints, brazed with the filler material of the.

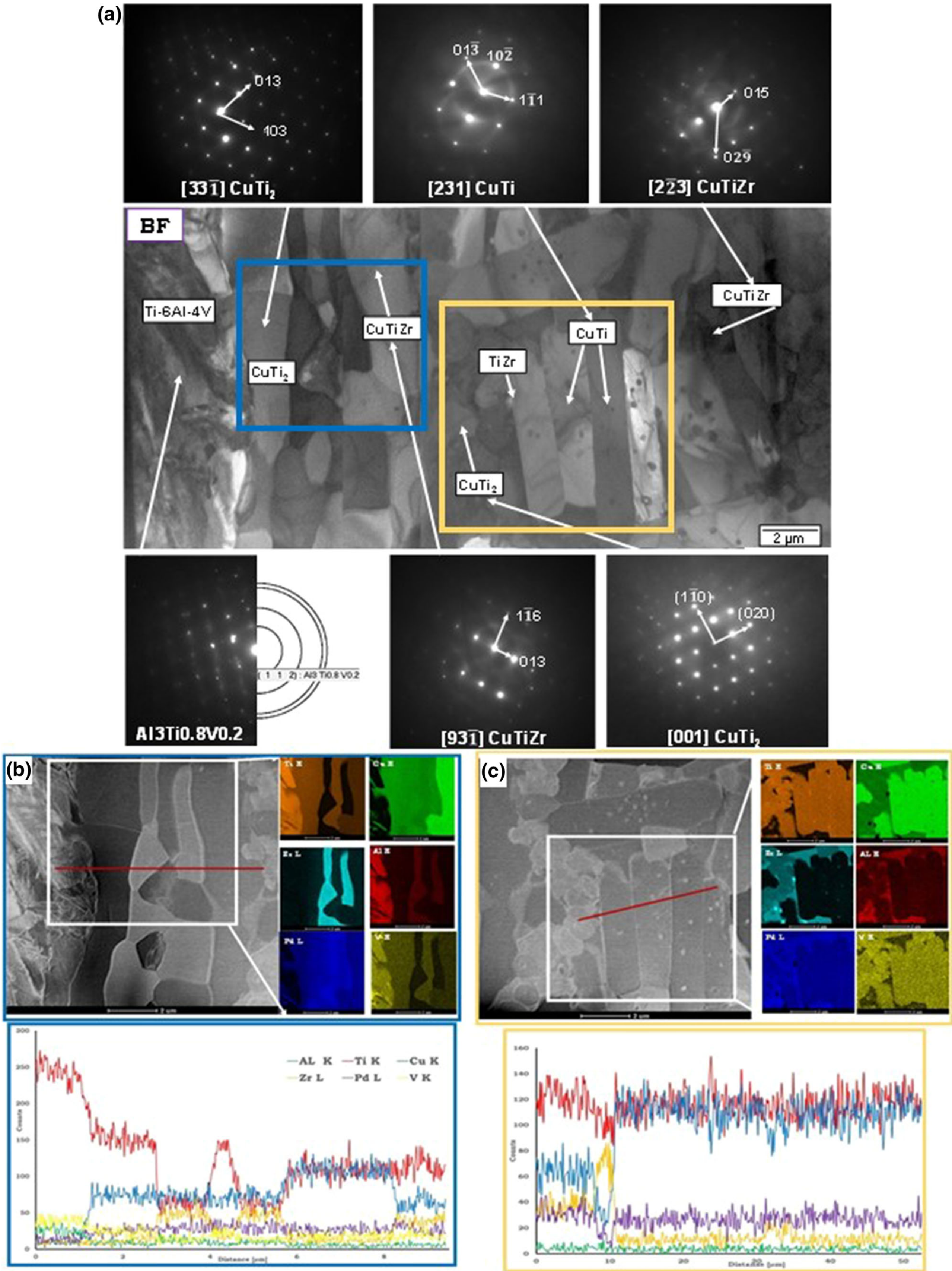

Fig. 4 Microstructure of the interface of the Ti-6Al-4 V/TiCiZrPd joint obtained by induction heating at 850 °C for 5 min: (a) TEM images, bright-field (BF) and corresponding SAED patterns, (b) TEM images, STEM-HAADF, map of elements distribution and line scan at the substrate side interface, (c) TEM images, STEM-HAADF, map of elements distribution and line scan in the central part of the joint

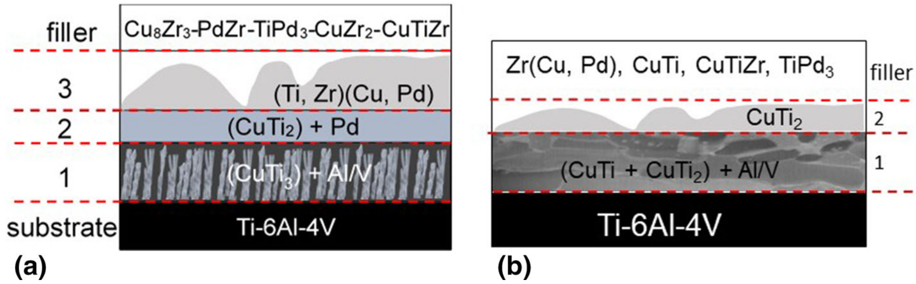

Fig. 5 Diagram of the formation of intermetallic phases in the joint obtained using (a) resistance heating, (b) induction heating

Ti(Zr)Cu-Ni-(Pd) composition are strongly dependent on the microstructure of the brazing zone. Especially, the formation of the brittle intermetallic phase in the center of the brazing zone, reduces the mechanical strength of the joints. Tensile tests of the brazed Ti-6Al-4 V and CPTi joints revealed that these joints exhibit excellent mechanical properties, even comparable to those of the base metal joints, provided that the brazing zone is free of the brittle intermetallic phases such as λ-Cu2TiZr and Laves-type phases (Ref 32).

The results achieved allowed to propose the diagram of the phases formed at the substrate/filler reaction zone (Fig. 5). The changes in the number of reaction layers and their chemical composition in the joint were observed in both cases. After the resistance heating, the layer noted as 1 was formed by the bright needles of $CuTi_3$ phase imposed in the matrix of the substrate composition. The formation of the $CuTi_3$ phase may result from the solid-state eutectoid reaction during cooling: β-Ti $\rightarrow$ α-Ti + $CuTi_3$. On the other hand, after induction heating, the layer 1 was composed of alternately arranged CuTi and $CuTi_2$ phases. On the contrary, after resistance brazing, the layer 2 was not observed. The microstructure in the middle of the joint was multiphase, but after induction brazing, it was less compex and the intermetallic layer was thinner. This diagram can be useful for designing the brazing process of titanium alloys to get the appropriate joint structure.

3.2 Characterization of Mechanical Properties and Phenomena Occurring in Joints Under Shearing Stresses

The joints were also subjected to the shear tests at room temperature. Analysis the effect of brazing temperature on the shear strength revealed its increase in the joints formed after induction brazing. This showed that the use of induction brazing increases the shear strength of the tested joints by two to three times (Fig. 6). After induction brazing, the shear strength was about 120 MPa. The highest shear strength of 610 MPa was obtained for temperature 850 °C. In comparison, for the joint achieved by the resistance brazing at 810 °C, the shear strength was 21 MPa. For this heating method, increasing the brazing temperature to 850 °C caused a double decrease in the shear strength to 12 MPa. Thus we may conclude that the induction brazing significantly increased the shear strength of the obtained joints what is related to the width of the diffusion zone at the interface.

Figure 6 presents the structure of the fracture surface of the joint after its shear test. The characterization of the obtained fractures using scanning electron microscopy showed that during the brazing process, the use of the induction heating eliminated voids formation in the joint. In this case the ductile fractures (Fig. 7b), composed of many dimples (craters) of different sizes and shapes were observed. The number, size and shape of these craters depend on the chemical composition and stereological parameters of the phases formed in the joint. The increasing contribution of plastic deformation to the fracture process is exhibited by the increase in ripples, extension of the edges of the cleavage ridges, formation of the deformed deep holes and areas of depressions (dimples, voids), characteristic for the ductile or plastic fracture. On the other hand, a quasi-brittle fracture type was observed for the joints obtained by the resistance heating, which reveal features typical for the brittle and ductile fracture (Fig. 7a). Quasi-cleavage material separation occurred upon nucleation of the brittle fracture in the local areas and their propagation to the surface causing decohesion, by inducing the plastic deformation mechanism. As a result of this deformation, fracture ridges with rough edges were formed. This fracture structure indicates a large plastic deformation during their formation.

Yue et al. (Ref 33) and Peng et al. (Ref 34) observed a similar character of the fracture structure during brazing of titanium alloys. Yue et al. (Ref 33) used an alloy with Ag for brazing. In this study, shear tests on brazed specimens showed that the fractures occurred in the Ag-rich phase, indicating a ductile fracture type. When the brazing temperature was increased to 980 °C, a large amount of Ag-rich phase was depleted from the joint and the fractures occurred in the $CuTi_2$ and in the Ti-Cu-rich phases. However, the shear strength decreased to 123 MPa. In contrast, Chang and Shiue (Ref 35) showed by the infrared technique that the average shear strength of a sample brazed at 970 °C for 180 s was 251 MPa. The joint failure was localized at the braze alloy, and a quasi-cleavage crack with slide marks on the facets was commonly observed on the broken surface. An analysis of the literature indicates that the use of lower brazing temperature and amorphous film with Pd as a metal filler can assure acceptable strength for the joints of Ti alloys.

4. Conclusions

The brazing process with the use of the amorphous filler was investigated. The following conclusion could be drawn:

1) The applied Ti-Cu-Zr-Pd amorphous alloys as a filler metal allowed to obtain stable, homogeneous, defect-free joints without the use of a flux, and they can be used successfully both for conventional and induction brazing,

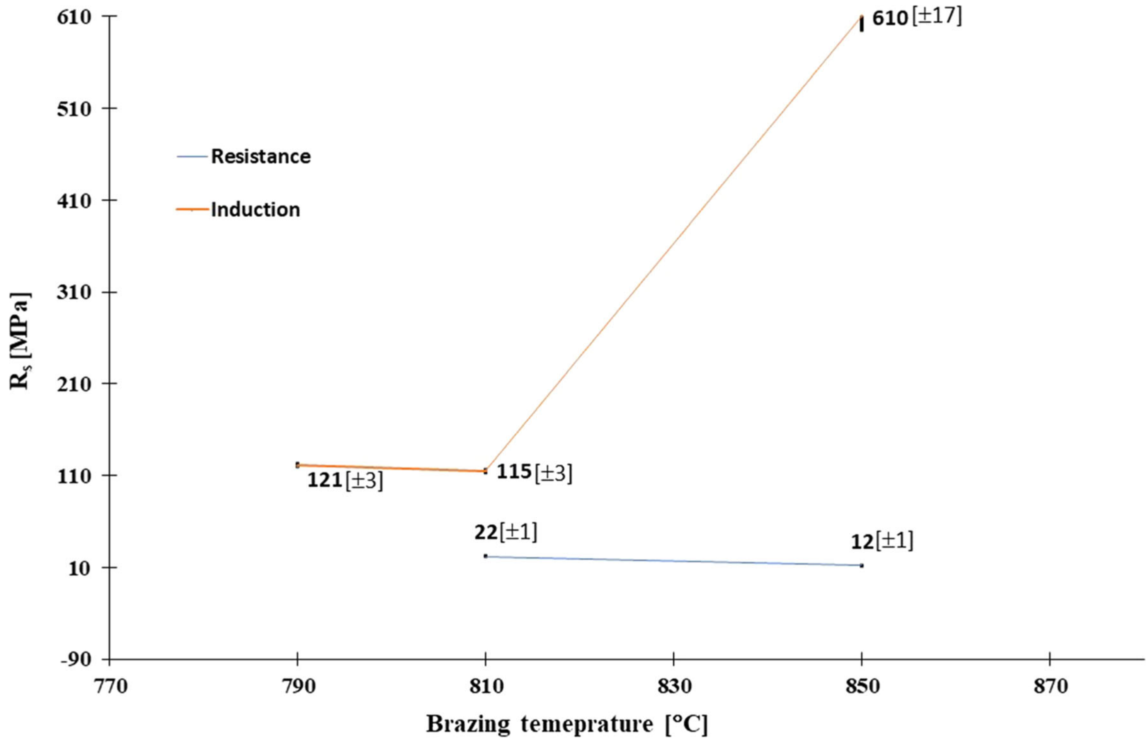

Fig. 6 Evaluation of joint shear strength depending on the heating method and temperature applied for brazing

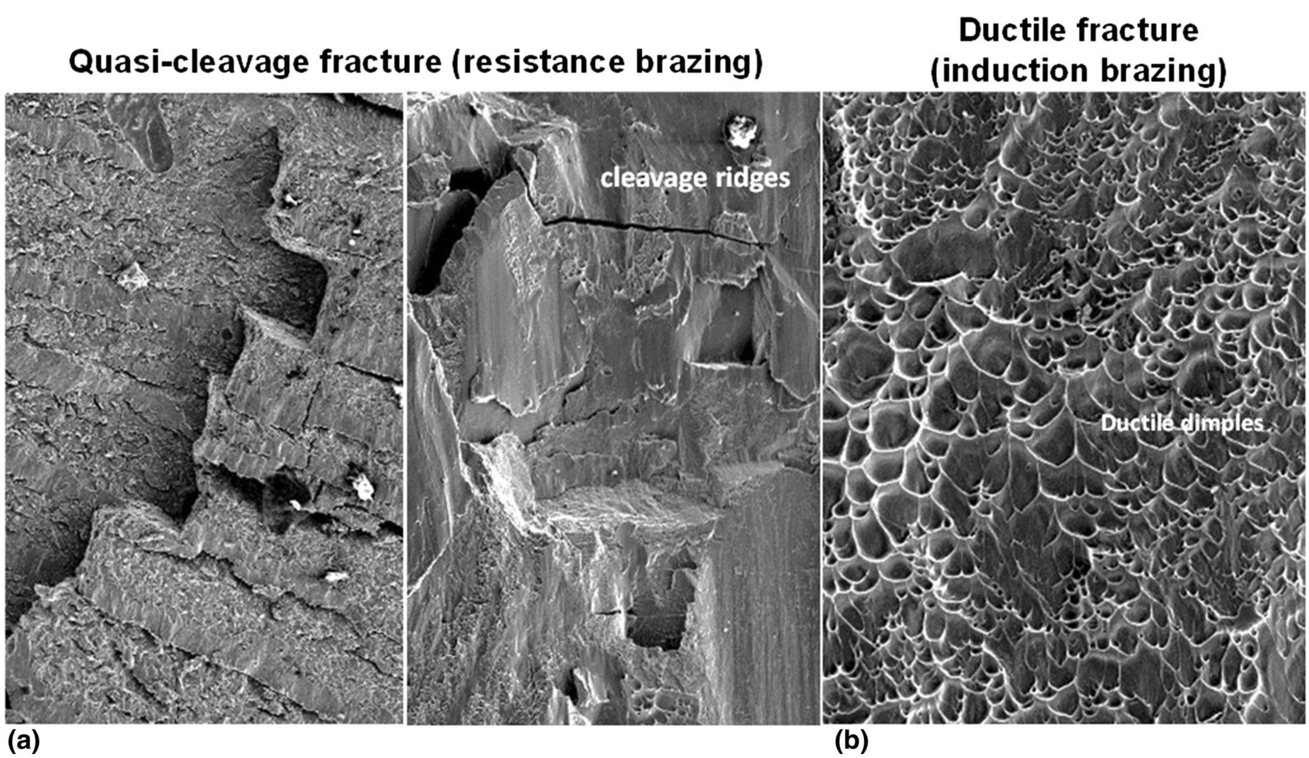

Fig. 7 SEM images showing the morphology of the fracture after the shear test of the joint obtained by: (a) resistance heating, (b) induction heating

2) Both resistance and induction heating allowed to obtain Ti-6Al-4 V/TiCuZrPd/ Ti-6Al-4 V joints with a very good properties,
3) The proposed model of the reaction zone structure assumes the existence of the following interfacial phases:—(1) $CuTi_3$(Al/V), (2) $CuTi_2$(Pd), (3) (Ti,Zr)(Cu,Pd) in the resistance brazing, and—(1) CuTi—$CuTi_2$(Al/V), (2) $CuTi_2$(Pd) phases in the case induction brazing, the microstructure in the central part of the joint is multiphase,
4) The use of induction heating for brazing strongly increased the shear strength of the tested joints and it is related to the decreased width of the diffusion zone formed at the substrate/filler material interface,
5) After induction brazing, the joints exhibited a ductile failure while fractured surfaces had many dimples of different sizes and shapes,
6) After resistance brazing, the joints showed a quasi-brittle type of fracture accompanied with quasi-cleavage separation of material through the nucleation of the brittle fracture in the local areas propagating to the surface.

Acknowledgments

The work was financed within the Project no UMO-2013/11/B/ST8/04286 by the National Science Centre of Poland and accomplished in the Accredited Laboratories of IMIM PAS in Krakow as a statutory project in years 2019-2022. The author would like to thank Dr. B. Madejski from the Institute of Aviation, Warsaw, Poland for his assistance in the performance of the shear tests.

References

1. E. Ganjeh, H. Sarkhosh, M.E. Bajgholi, H. Khorsand, and M. Ghaffari, Increasing Ti-6Al-4V Brazed Joint Strength Equal to the Base Metal by Ti and Zr Amorphous Filler Alloys, *Mater. Charact.*, 2012, **71**, p 31–40
2. B. Komolafe, A Study on the Wetting Behaviour of Ti-20Zr-20Cu-20Ni Brazing Filler on Ti-6Al-4V, MSc Thesis, Concordia University, Canada, 2014, http://spectrum.library.concordia.ca/979192
3. X.G. Song, J. Cao, H.Y. Chen, Y.F. Wang, and J.C. Feng, Brazing TiAl Intermetallics Using TiNi-V Eutectic Brazing Alloy, *Mater. Sci. Eng. A*, 2012, **551**, p 133–139
4. I.-T. Hong and C.-H. Koo, Microstructural Evolution and Shear Strength of Brazing C103 and Ti-6Al-4V Using Ti-20Cu-20Ni-20Zr (wt.%) Filler Metal, *Int. J. Refract. Met. Hard Mater.*, 2006, **24**, p 247–252
5. M.K. Lee, J.G. Lee, K.H. Kim, C.H. Lim, C.K. Rhee, and C.H. Park, Amorphous Sputter Coating of a Multi-Component Zr-Ti-Ni-Cu Alloy as a Filler for Brazing Zircaloy-4, *J. Nucl. Mater.*, 2012, **426**, p 9–15
6. S. Pang, L. Sun, H. Xiong, C. Chen, Y. Liu, H. Li et al., A Multicomponent TiZr Based Amorphous Brazing Filler Metal for High-Strength Joining of Titanium Alloy, *Scripta Mater.*, 2016, **117**, p 55–59
7. T. Onzawa, A. Suzumura, and M.W. Ko, Brazing of Titanium Using Low-Melting-Point Ti Based Filler Metals, *Welding R.*, 1990, **69**(12), p 462–467
8. Y. Jing, D. Su, X. Yue, T.B. Britton, and J. Jiang, The Development of High Strength Brazing Technique for Ti-6Al-4V Using TiZrCuNi Amorphous Filler, *Mater. Character.*, 2017, **131**, p 526–531
9. E.Y. Ivanov, A.E. Shapiro, and M.G. Horne, Exploring Solid-State Synthesis of Powder Filler Metals for Vacuum Brazing of Titanium Alloys, *Weld. J.*, 2006, **85**, p 196–199
10. A. Muhrat, H. Puga, and J. Barbosa, Low-Temperature Brazing of Titanium Using Al Based Filler Alloys, *Adv. Mater. Sci. Eng.*, 2018, **2**, p 1–16
11. C.T. Chang, Y.C. Du, R.K. Shiue, and C.S. Chang, Infrared Brazing of High-Strength Titanium Alloys by Ti-15Cu-15Ni and Ti-15Cu-25Ni Filler Foils, *Mater. Sci. Eng. A*, 2006, **420**(1–2), p 155–164
12. Y.C. Du and R.K. Shiue, Ti-6Al-4V Using Two Silver-Based Braze Alloys, *J. Mater. Process. Technol.*, 2009, **209**, p 5161–5166
13. L. Li, KHu. X-q Li, B. He, and H. Man, Brazeability Evaluation of Ti-Zr-Cu-Ni-Co-Mo Filler for Vacuum Brazing TiAl-Based Alloy, *Trans. Nonferrous Met. Soc. China*, 2019, **29**, p 754–763
14. M.K. Lee and J.G. Lee, Mechanical and Corrosion Properties of Ti-6Al-4V Alloy Joints Brazed with a Low-Melting-Point 62.7Zr-11.0Ti-13.2Cu-98Ni-33Be Amorphous Filler Metal, *Mater. Char.*, 2013, **81**(4), p 19–27
15. Y. Wang, X.Q. Cai, Z.W. Yang, D.P. Wang, X.G. Liu, and Y.C. Liu, Diffusion Bonding of Ti2AlNb Alloy Using Pure Ti Foil as an Interlayer, *J. Alloy. Compd.*, 2018, **756**, p 163–174
16. X.G. Song, J. Cao, H.Y. Chen, H.Q. Wang, and J.C. Feng, Contact Reactive Brazing of Ti53311S Alloy Using Cu Foil as Interlayer: Interfacial Microstructure and Joining Properties, *Mater. Des.*, 2013, **46**, p 895–901
17. W. Guo, J. Xue, H. Zhang, H. Cui, Y. Zhu, P. Peng, and B. Qi, The Role of Foam on Microstructure and Strength of The Brazed C/C Composites/Ti6Al4V Alloy Joint, *Vacuum*, 2020, **179**, p 109543
18. A. Shapiro and A. Rabinkin, State of the Art of Titanium-Based Brazing Filler Metals, *Welding J.*, 2003, **83**(10), p 36–43
19. Y. Jing, D. Su, X. Yue, T. Ben Britton, and J. Jiang, The Development of High Strength Brazing Technique for Ti-6Al-4V Using TiZrCuNi Amorphous Filler, *Mater. Charact.*, 2017, **131**, p 526–531
20. Y. Zhang, W.G. Zhang, J.P. Lin, G.J. Hao, G.L. Chen, and P.K. Liaw, Glass-Forming Ability and Competitive Crystalline Phases for Lightweight Ti-Be-Based Alloys, *Metall. Mater. Trans. A*, 2010, **41**, p 1670–1676
21. S. Zin and S.L. Semiatin, *Elements of Induction Heating: Design, Control, and Applications*, ASM International, Almere, Netherland, 1988
22. M.J. Donachie, *Titanium: A Technical Guide*, 2nd ed. ASM International, OH, USA, 2000
23. P. Roberts, *Industrial Brazing Practice*, 2nd ed. CRC Press Boca Raton, Florida, 2013
24. Y. Matychak, I. Pohrelyuk, V. Fedirko, and O. Tkachuk, Modelling of Microstructural Evolution of Titanium During Diffusive Saturation by Interstitial Elements, *Titanium Alloys-Adv Proper Control*, 2013 https://doi.org/10.5772/49999
25. A. Sypien and W. Przybylo, Preparation of the Phase TiNiFe by the Levitation and Its Structural Characterization, *J. Mater. Sci. Technol.*, 2010, **26**, p 31–35
26. A. Sypien, T. Czeppe, G. Garzel, L. Litynska-Dobrzynska, J. Latuch, and N.Q. Chinh, Thermal Stability and Mechanical Properties of the TiCuZrPd Glasses with 10, 14 and 20 at.% Pd, *J. Alloy. Compd*, 2014, **615**, p 108–112
27. A. Sypien, K. Badura, P. Fima, and K. Miernik, Effect of Pd, Temperature and Time on Wetting and Interfacial Microstructure of Bulk Metallic Glasses TiCuZrPd on Ti-6Al-4V Substrate, *J. Alloy. Compd*, 2017, **695**, p 962–970

28. A. Sypien, M. Stoica, and T. Czeppe, Properties of the Ti_{40}-$Cu_{36}Zr_{10}Pd_{14}$ BMG Modified by Sn and Nb Additions, *J. Mater. Eng. Perform.*, 2016, **25**, p 800–808
29. T. Czeppe, A. Sypien, and A. Wierzbick-Miernik, Modification of the Ti40Cu36Zr10Pd14 BMG Crystallization Mechanism with Heating Rates 10-140 K/min, *J. Mater. Eng. Perform.*, 2016, **25**, p 5289–5301
30. E. Lugscheider and L.M. Ruiz, *Brazing of Titanium International Conference on Advances in Joining and Cutting Processes*, Abington Publishers, Harrogate, UK, 1989, p 414–423
31. E. Lugscheider and U. Broich, Mechanical Properties of High-Temperature Brazed Titanium Materials, *Weld. J.*, 1995, **74**, p 169–176
32. E. Lugscheider and L. Martinez, Development of New Ti-Base Filler Metals for Ti6Al4V, DVS Berichte Bd 132, DVS-Verlag, (2004)
33. X. Yue, P. He, J.C. Feng, J.H. Zhang, and F.Q. Zhu, Microstructure and Interfacial Reactions of Vacuum Brazing Titanium Alloy to Stainless Steel Using an AgCuTi Filler Metal, *Mater. Charact.*, 2008, **59**, p 1721–1727
34. Y. Peng, J. Li, Y. Du, and J. Xiong, J Shi 2021 Microstructure and Mechanical Properties of Joints Prepared by Vacuum Brazing on TC_4 Titanium Alloy with Ag As Filler Metal, *Vacuum*, 2021, **187**, p 110134
35. C.T. Chang and R.K. Shiue, Infrared Brazing Ti-6Al-4V and Mo Using the Ti-15Cu-15Ni Braze Alloy, *Int. J. Refract. Met. Hard Mater.*, 2005, **23**, p 161–170